Biosensors and Bioelectronics 54 (2014) 541–546

Contents lists available at ScienceDirect

Biosensors and Bioelectronics

journal homepage: www.elsevier.com/locate/bios

Sensitive and selective real-time electrochemical monitoring of DNA repair

Marc A. McWilliams [a], Fadwa H. Anka [b], Kenneth J. Balkus [b], Jason D. Slinker [a,*]

[a] Department of Physics, The University of Texas at Dallas, 800 W. Campbell Road, EC 36, Richardson, TX 75080, USA
[b] Department of Chemistry, The University of Texas at Dallas, 800 W. Campbell Road, BE 26, Richardson, TX 75080, USA

ARTICLE INFO

Article history:
Received 24 August 2013
Received in revised form
24 October 2013
Accepted 10 November 2013
Available online 15 November 2013

Keywords:
Electrochemical sensor
DNA repair
8-oxoguanine
Biosensor
Base-excision repair
Oxidative damage

ABSTRACT

Unrepaired DNA damage can lead to mutation, cancer, and death of cells or organisms. However, due to the subtlety of DNA damage, it is difficult to sense the presence of damage repair with high selectivity and sensitivity. We have shown sensitive and selective electrochemical sensing of 8-oxoguanine and uracil repair glycosylase activity within DNA monolayers on gold by multiplexed analysis with silicon chips and low-cost electrospun nanofibers. Our approach compared the electrochemical signal of electroactive, probe-modified DNA monolayers containing a base defect versus the rational control of defect-free monolayers. We found damage-specific sensitivity thresholds on the order of femtomoles of proteins and dynamic ranges of over two orders of magnitude for each target. Temperature-dependent kinetics were extracted, showing exponential signal loss with time constants of seconds. Damage specific detection in a mixture of enzymes and in response to environmental oxidative damage was also demonstrated. Nanofibers were shown to behave similarly to conventional gold-on-silicon devices, showing the potential of these low-cost devices for sensing applications. This device approach achieves a sensitive, selective, and rapid assay of repair protein activity, enabling a biological interrogation of DNA damage repair.

1. Introduction

DNA is constantly subject to damage from endogenous and exogenous factors that threaten the vitality of cells and the integrity of the genome. Left unchecked, this damage can give rise to unregulated cell division leading to cancerous tumors (David et al., 2007; Kunkel and Erie, 2005; Sancar et al., 2004). From a chemical standpoint, DNA damage is very subtle. For example, 8-oxoguanine, the most prevalent oxidative DNA damage product, involves the addition of a single oxo-bond, yet this moiety has drastic consequences for DNA replication and genomic stability (Obtułowicz et al., 2010; Maehara et al., 2008). To address damage such as this, cells are equipped with an intricate repair pathway to counteract the devastating proliferative effects of DNA damage (David et al., 2007; Kunkel and Erie, 2005; Sancar et al., 2004). For the first step in this pathway, various DNA glycosylases recognize and excise damage products. Study of this crucial step should have great consequences in cancer research, but to date, the connection of deficiencies in repair proteins to cancer has remained elusive, in part due to overlapping functionalities of repair glycosylases (Paz-Elizur et al., 2008). A biological assay that could follow repair at the level of the subtle DNA damage site would greatly assist the understanding of damage repair and potentially lead to new insight into the connection of DNA repair pathways and cancer.

The challenge in detecting DNA repair is tied to the difficulty of selectively distinguishing removal of subtle base defects. Achieving this selectivity in a stand-alone device for convenient assay and low-cost clinical detection is highly advantageous. 8-oxoguanine itself has been distinguished by GC–MS and HPLC-coupled electrochemical detection, but these techniques require digestion of the DNA and are not compatible with real-time quantitative analysis of protein activity (Abalea et al., 1999; Ivandini et al., 2007; Ravanat et al., 1998; Rebelo et al., 2004). Electrochemical devices have been used to indirectly study DNA damage. Cahová-Kuchaříková et al. (2005) detected UV-induced pyrimidine dimer formation in supercoiled DNA by treating with T4 endonuclease and directly detecting the end-termini of resulting single strand breaks and release of single stranded DNA. Havran et al. (2008) detected DNA damage products similarly extracted from supercoiled DNA with an osmium marker specific to single-stranded DNA. Wang et al. (1997) followed the formation of 8-oxoguanine on DNA-modified carbon electrodes by following the loss of undamaged guanine signal. Similarly, the electrochemically-induced generation of 8-oxoguanine and 8-oxoadinine was studied by Harfield et al. (2011) on nickel-modified boron-doped diamond

* Corresponding author. Tel.: +1 972 883 6513.
E-mail address: slinker@utdallas.edu (J.D. Slinker).

0956-5663/$ - see front matter © 2013 Elsevier B.V. All rights reserved.
http://dx.doi.org/10.1016/j.bios.2013.11.034

electrodes. The group of Rusling has demonstrated a highly sensitive electrogenerated chemiluminescence 8-oxoguanine sensor (Dennany et al., 2004; Mugweru et al., 2004). Recently, an effective photoelectrochemical device was created for measuring 8-oxoguanine presence with good sensitivity and measure of post-repair changes in concentration (Zhang et al., 2012). Nanopore devices for location-specific oxidative damage reporting have been developed (Schibel et al., 2010). These techniques, however, have not offered real-time quantitative measure of repair activity.

Alternatively, to follow damage repair real-time in a stand-alone device, a recognition element capable of selectively distinguishing subtle damage products and an appropriate transduction pathway is needed. DNA is the natural recognition element for not only the binding of repair proteins but also their repair activity, and DNA can be synthesized with or without damage/lesion sites to establish controls. Furthermore, DNA can additionally serve as an electrical transducing element when modified with a redox-active probe and self-assembled on a working electrode (Paleček and Bartošík (2012)). Previous experiments have shown that DNA electrochemistry can be used to sense subtle DNA lesions and DNA-binding protein activity (Boal and Barton, 2005; Boon et al., 2000, 2002a; Zuo et al., 2009). Transduction of sensing involves a change in the efficiency of the oxidation or reduction of the redox probe due to a change in charge transport efficiency of the DNA bridge. DNA monolayers may be prepared with probes that interact directly with the electrode surface (Cash et al., 2009; Ricci et al., 2009; White and Plaxco, 2010; Zhang et al., 2012; Zuo et al., 2009) or involve charge propagation through the DNA bridge (Boal and Barton, 2005; Boal et al., 2005; Boon et al., 2000, 2002a, 2002b; Gorodetsky et al., 2006, 2008; Mui et al., 2011; Slinker et al., 2010). For the latter, charge transport through the DNA base pair π-stack enables sensitivity to single-base defects (Boal and Barton, 2005; Boon et al., 2000; Slinker et al., 2011). Along these lines, DNA electrochemistry has been used to study glycosylases, in large part to sense their presence through DNA-mediated electrochemical reduction of the 4Fe–4S cluster (Boal et al., 2005; Boon et al., 2002a; Boon et al., 2002b; Gorodetsky et al., 2008; Mui et al., 2011). However, the sensitivity, selectivity, and kinetics of DNA electrochemistry to repair protein activity have yet to be fully clarified. In particular, the quantitative real-time electrical detection of the repair of 8-oxoguanine, one of the most common oxidative damage products and a key factor in aging and cancer, has yet to be shown.

Here, we investigate the concentration and kinetics of DNA 8-oxoguanine and uracil repair glycosylase activity using selective DNA modified electrodes with rational control. This is accomplished through DNA electrochemistry with multiplexed electrodes on silicon chips and also with unconventional devices utilizing low-cost electrospun nanofibers. Using multiplexed analysis, we demonstrate the selectivity of our devices to damaged products against defect-free controls and observe the temperature-dependent rate of repair. We also investigate the use of electrospun fibers as low-cost alternative sensors.

2. Materials and methods

2.1. DNA preparation

The double stranded DNA monolayers utilized were from the 17mer sequence 3′-CTCTATATTTCGTGCGT$_{NB}$-5′ and the fully complementary sequence 5′-(C6 thiol)–GAGATATAAAGCACGCA-3′, where the underlined bases note the positions of an inserted uracil (T) or 8-oxoguanine (G), and T_{NB} notes the position of a Nile Blue modified thymine. The thiolated undamaged and uracil-containing DNA strands were purchased from Integrated DNA Technologies (IDT, USA) and was received cleaved from solid support and deprotected. The other strands were purchased from TriLink (USA). For the 8-oxoguanine strand, the 8-oxo-dG-CE phosphoramidite from Glen Research (product 10-1028-xx, USA) was incorporated at the specified position. This strand was deprotected in ammonium hydroxide with 0.25 M 2-mercaptoethanol 17 h at 55 °C to avoid degradation of 8-oxoguanine. For the Nile Blue modified strand, a 5-[3-acrylate NHS ester]-2'-deoxyUridine phosphoramidite (Glen Research) was incorporated at the 5' terminus by TriLink using ultramild synthesis conditions. The DNA on solid support was then dried and reacted with a 10 mg/mL solution of Nile Blue perchlorate (Acros Organics, USA) in 9:1 dichloromethane/N,N-diisopropylethylamine solution for approximately 24 h. Excess reagents were then removed by washing with dichloromethane, methanol, and acetonitrile. These Nile Blue modified DNA strands were then cleaved from the support and deprotected according to ultramild conditions with 0.05 M potassium carbonate in methanol at ambient temperature for 8 h.

Oligonucleotides were purified by high performance liquid chromatography (HPLC). Following HPLC purification of the products, the oligonucleotides were treated to remove the dimethoxytrityl (DMT) protecting group. For the thiolated oligonucleotides, the disulfide of the thiolated linker was cleaved with an excess of dithiothreitol in concentrated ammonium hydroxide for 2 h to yield the free thiol. The DMT was removed from the Nile Blue DNA strands by treating with an 80% solution of glacial acetic acid for 20 min, followed by quenching of the reaction with an excess of ethanol. All the oligonucleotides were dried and purified with a second round of HPLC. The products were characterized by HPLC, matrix assisted laser desorption ionization (MALDI) time-of-flight mass spectrometry, and UV-visible (UV–vis) spectrophotometry. The oligonucleotides were subsequently desalted and quantified by UV–vis spectrophotometry according to their extinction coefficients (IDT Oligo Analyzer). Duplexes were formed by thermally annealing equimolar amounts of oligonucleotides at 90 °C for 5 min in deoxygenated phosphate buffer (5 mM NaPhos, 50 mM NaCl, pH 7.0) followed by slow cooling to ambient temperature.

2.2. Silicon chip preparation

One millimeter thick Si wafers with a 10,000 Å thick oxide layer were purchased from Silicon Quest. Wafers were cleaned thoroughly in 1165 Remover (Microchem, USA) and vapor primed with hexamethyldisilizane (HMDS). SPR 220 3.0 photoresist (Microchem) was spin-cast at 4000 rpm and baked. The photoresist was patterned with a Karl Suss MA6 contact aligner and a chrome photomask. Following post exposure baking, wafers were developed in AZ 300 MIF (Microchem) developer for 1 min and rinsed thoroughly with deionized water. A 15 Å Ti adhesion layer and a 1000 Å Au layer were deposited on the chips with an electron beam evaporator. Wafers were then immersed in 1165 Remover overnight and sonicated as needed to complete metal lift-off. The wafers were thoroughly baked and cleaned by UV ozone treatment. Subsequently, SU-8 2002 (Microchem) was spin-cast at 3000 rpm, baked, and photopatterned as above. Wafers were developed in SU-8 Developer (Microchem) for 1 min and baked for a permanent set of the photoresist. The wafers were subsequently diced into 1-in. by 1-in. chips by hand with a diamond scribe and stored under vacuum until use.

2.3. Electrospun fiber preparation

Polyacrylonitrile (150,000 MW, PAN) was purchased from Pfaltz and Bauer (USA). Dimethylformamide (DMF), hydroxylamine hydrochloride ($NH_2OH \cdot HCl$) and gold(III) chloride hydrate

($HAuCl_4 \cdot H_2O$) were purchased from Aldrich (USA). The electrospinning solution was prepared by combining 9 mL of DMF with 1 g of PAN followed with stirring at 80 °C for 2 h. After the PAN solution cooled to room temperature, 5 mL of the PAN solution was added to 0.03 g of $HAuCl_4$ to make a 0.022 M solution and was stirred for 3 h. Electrospinning was conducted using a flow rate of 0.1 mL/h and voltage 11 kV while distance between the needle and collector was 15 cm.

The electrospun PAN/Au^{3+} sheet was coated with gold according to a previously reported procedure with some modifications (Han et al., 2006; Liu et al., 2011; Zhao et al., 2008). The fiber sheet was placed on a filter paper and 200 ml solution of sodium borohydride $NaBH_4$ (1 mM, 0.0076 g) was filtered ten times through the sheet using suck filtration in order to reduce the gold ions inside the fibers. The sheet was rinsed with 0.1 M HCl then deionized water repeatedly and was then placed in a Petri dish and covered with $HAuCl_4$ solution (17 ml, 0.0026 M) before being inserted into a Rayonet UV reactor containing eight 254 nm UV lamps (RMR-2537) for 2 h. After 2 h, the sheet was purple in color indicating that Au nanoparticles are immobilized on the fibers. It was then left to dry out at ambient temperature. A solution of 0.02 g $HAuCl_4$, 4 mg NH_2OH, and 200 ml DI water was filtered through the sheet repeatedly until the solution turned clear. This process was repeated until the sheet turned golden brown indicating that the fibers were well coated. The electrospun fiber sheet was cut into strips and placed on a glass slide. Outside of the well, silver contact pads were painted onto the slide to further immobilize the fibers.

2.4. Sensor device assembly

The DNA was assembled on either the silicon chips bearing 16 gold electrodes or the electrospun polyacrylonitrile mats enhanced with gold nanoparticles. To secure an enzyme bearing solution over these devices and to hold the fiber strip in place, a rubber gasket and clamp assembly was used. The clamp enabled assembly of up to four distinct sequences on a given device. These devices supported the assembly and interrogation of both defect-free and defect-bearing monolayers on the same device platform and in the same enzyme-bearing solution for study of protein activity versus a negative control. Sequences of 25 μM duplex DNA solutions in phosphate buffer were assembled on these devices in a humidified environment for a period of 16–20 h. Upon completion of film formation, the devices were backfilled with 0.5 mM 1-mercaptohexanol in a 95:5 phosphate buffer/glycerol solution for 60 min. The electrodes and cells were rinsed thoroughly prior to electrochemistry experiments to ensure removal of residual alkanethiols.

2.5. Electrochemical measurements and enzyme handling

Electrochemical measurements were performed with a CH Instruments (USA) CHI750 electrochemical analyzer and a CHI684 multiplexer module. DNA repair glycosylases were purchased from New England BioLabs (USA) and exchanged to the electrochemistry buffer with a Pierce Slide-A-Lyzer mini dialysis kit. Electrochemical analysis of formamidopyrimidine-DNA glycosylase (FPG) was performed in pH 7.9 buffer containing 50 mM NaCl, 10 mM Tris–HCl, 10 mM $MgCl_2$, and 4 mM spermidine. Electrochemical analysis of uracil DNA-glycosylase (UDG) was performed in pH 8.0 buffer 20 mM Tris–HCl, 1 mM ethylenediaminetetraacetic acid (EDTA), 4 mM $MgCl_2$, and 4 mM spermidine. Stock molar concentrations of FPG (16.5 μM) and UDG (1.97 μM) were obtained from direct communication with New England Biolabs.

3. Results and discussion

3.1. Detector configuration and approach

Fig. 1 illustrates our approach in electrochemically detecting the activity of these proteins. We prepared DNA monolayers incorporating 8-oxoguanine defects or single uracil defects and studied the repair activity of formamidopyrimidine-DNA glycosylase (FPG), an 8-oxoguanine DNA glycosylase, and uracil DNA-glycosylase (UDG). FPG releases the damaged guanine and cleaves both the 3′ and 5′ ends of the abasic site, leaving a gap in the sugar–phosphate backbone. UDG executes glycosylase activity by hydrolyzing the uracil and extracting it without cutting the

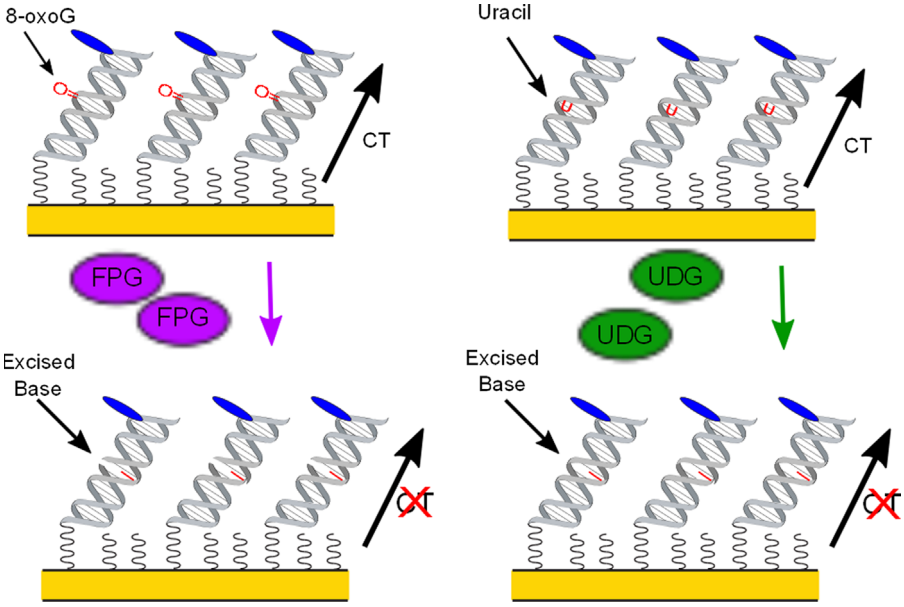

Fig. 1. Illustration of glycosylase repair protein activity. Well-matched, fully base paired DNA monolayers on gold facilitate charge transport (CT) to an electrochemical redox probe. Repair proteins recognize damage products and lesions, such as 8-oxoguanine and uracil, removing the affected base. The excision of this base decreases charge transport to the probe.

backbone. These actions disrupt the π-stack and attenuate charge transport (CT) between the electrode and distally bound redox probe. A damage-free control will not show this activity, allowing us to properly quantify the effect of the repair action apart from nonspecific protein binding.

Beginning with silicon chips bearing 16 gold electrodes (2 mm^2), we explored the damage-specific detection of DNA repair glycosylase activity. These repair proteins bind to DNA nonspecifically but excise their target bases with high specificity. Therefore, we prepared our chips with both lesion-containing and undamaged monolayers (Fig. 2A) as a control for proper signal normalization, as the DNA-binding event itself can affect the charge transport efficiency. This ability to present rational controls is a distinct advantage of DNA electrochemistry with multiplexed analysis. We measured the square wave voltammetry of these monolayers and characterized the protein activity by the peak height of the Nile Blue redox signal. Sample volumes typically ranged from 200 to 400 μL. Fig. 2B shows the square wave voltammograms of undamaged and 8-oxoguanine monolayers before (thin trace) and after (thick trace) addition of 100 units/mL of FPG. Before addition of FPG, both devices have comparable square wave peak signals associated with the Nile Blue redox probe, indicating efficient transport of charge through the DNA bridge. However, upon treatment with 100 units/mL of FPG, the square wave peak of the 8-oxoguanine monolayer is significantly attenuated (65% signal loss), consistent with the loss of a base from the DNA bridge, while the undamaged monolayer square wave peak retains substantially more peak height (19% signal loss). In both cases, the background of the voltammogram is changed, likely due to increased surface passivation by nonspecific binding of the glycosylase to both monolayers. Along these lines, a simple impedance assay presumably would not distinguish this activity as the binding of the glycosylase is indiscriminate. Alternatively, the square wave redox peak provides quantitative sensitivity to the excision event due to the removal of a base from the DNA bridge. Furthermore, though this enzyme has a suggested usage concentration of 1000 units/mL (16.5 μM FPG), our devices distinguish their activity at much lower concentrations.

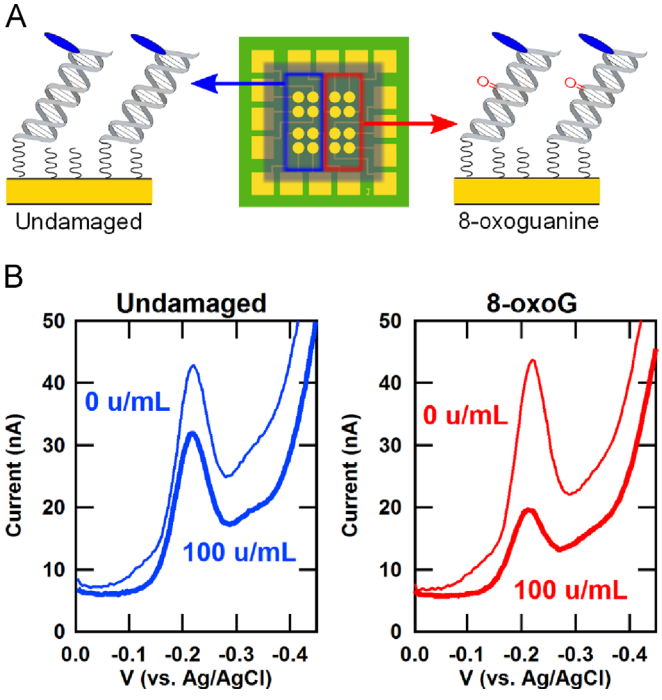

Fig. 2. (A) Illustration of the chip setup for damage-specific detection of glycosylase activity with undamaged and 8-oxoguanine damaged DNA monolayers. (Similarly arranged chips were used to study uracil incorporation.) (B) Square wave voltammograms of chip-bound undamaged (left, blue) or 8-oxoguanine damaged (right, red) DNA monolayers before treatment with formamidopyrimidine-DNA glycosylase (FPG) and after addition of 100 units/mL of FPG, respectively. (For interpretation of the references to color in this figure legend, the reader is referred to the web version of this article.)

To find the limits of detection of the 8-oxoguanine and uracil DNA monolayers to FPG and UDG, respectively, we obtained the response of our devices at various concentrations of these glycosylases (Fig. 3). For UDG, discernible signal loss over standard deviation is seen at 50 units/mL for a uracil-containing monolayer over a control. This corresponds to 20 nM, or 270 fmol of UDG per electrode on our chip. For FPG, the sensitivity is even greater, as low as 1–2 units/mL, 2–4 nM, or 35–70 fmol of FPG per electrode. This latter figure corresponds to approximately 1 FPG molecule per 25 DNA strands at the surface, with the surface coverage estimated from bottom bound redox probe electrochemistry with no Mg^{2+} used in assembly (Wohlgamuth et al., 2013). Each sensor shows a dynamic range over two orders of magnitude of glycosylase concentration, with a sensitivity of ~30%/decade. For FPG, the differential signal change saturates above 100 units/mL; thus, it essentially performs as a digital sensor at higher FPG concentrations. This demonstrates the high sensitivity and discernment of these sensors to glycosylase activity.

In addition, we also investigated the concentration-dependence of repair of 8-oxoguanine by FPG in the presence of 500 units/mL UDG (Supplemental data Fig. 1). This is a significant challenge to the assay, as UDG binds nonspecifically. Compared to UDG-free conditions, damage specific detection is inhibited at lower concentrations, but is clearly observed by FPG at 20 units/mL (40 nM, 700 fmol/electrode) and above, likely corresponding to a sufficient concentration to competitively dissociate UDG. We have also observed (Supplemental data Fig. 2) repair of induced DNA damage, specifically oxidative damage by the Fenton reagent (2 mM $FeCl_3$ and 1 mM H_2O_2) versus a control. Thus, damage specific detection can be achieved in mixtures of enzymes and in response to environmental oxidative damage.

Electrochemical monitoring of repair activity with DNA monolayers shows the timescale of repair activity. Notably, as we are utilizing the natural repair substrate as the recognition element, the transduction response gives a direct assay of the timescale of the biological activity. This allows us to understand differences in operating our electrochemical sensor at room temperature (22 °C) versus body temperature (37 °C), the ideal temperature for repair protein activity. Operation near 0 °C is also given as this is near the minimum temperature permitted by the protein buffer. Fig. 4 shows the temperature-dependent repair activity of FPG as measured by square wave voltammetry peak height at conventional FPG reaction concentration of 1000 units/mL. As can be seen, temperature has a dramatic influence on decay rates, with exponential decay parameters of 30 s, 6.5 s, and < 2.5 s for 0 °C, 22 °C,

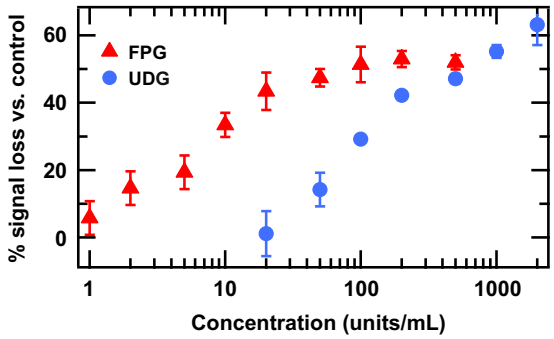

Fig. 3. SW peak current signal loss of chip-bound DNA monolayers containing uracil or 8-oxoguanine relative to an undamaged control versus concentration of UDG or FPG, respectively. Error bars represent the standard deviation over three independent experiments.

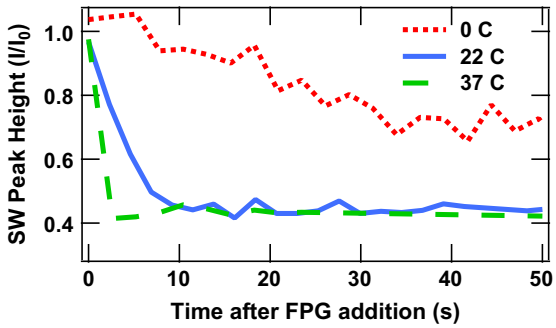

Fig. 4. SW peak current (40 Hz) height versus time after FPG addition, showing the real-time activity of FPG on 8-oxoguanine-bearing DNA monolayers.

and 37 °C, respectively. Given these decay times, these sensors can respond to excision changes on the order of seconds. Thus, sensing can be accomplished with great expediency, and electrochemical sensing permits a real-time measure of repair activity.

Finally, we demonstrate sensing from meshes of electrospun polymer nanofibers. This approach is beneficial for the construction of low cost sensors, as these fibers involve no photo- or electron beam lithography and no vacuum processing steps (Bellan and Craighead, 2011). Electrospinning is an easy and versatile bench top technique that allows the production of fibers with diameters ranging from a few micrometers to tens of nanometers. An electrospinning setup usually consists of a syringe pump, high voltage supply and a grounded collector. Typically, a high voltage is applied to a polymer solution within the syringe, resulting in a polymer jet ejected toward the collector as the electrostatic forces overcome the surface tension. The polymer jet dries on the way to the collector where nanofibers are deposited. Besides their ease of fabrication, their high surface area, and their low cost, electrospun nanofibers can be easily functionalized to be used in biosensors. Electrospun nanofibers used in detecting glucose (Manesh et al., 2008; Ren et al., 2006), cholesterol (Shin and Kameoka, 2012), pathogens (Luo et al., 2010) and proteins (Kunduru et al. 2010; Wang et al., 2012) have been reported. In particular, gold embedded electrospun nanofibers for use in different types of sensing have been demonstrated (Marx et al., 2011; Liu et al., 2011). However, immobilizing DNA on gold/polymeric electrospun nanofibers and their use in electrochemical sensing of DNA repair processes have yet to be explored.

We utilize polyacrylonitrile fibers coated with gold nanoparticles and assemble thiolated DNA on these fibers (Anka et al., 2012). Thus, the fibers themselves become the working electrode of the sensors, modified with either the lesion-bearing or defect-free DNA monolayers. Fig. 5 provides an illustration of these fibers as well as an SEM image of these constructs. SEM analysis reveals that fibers with average diameters of 900 nm were produced with high gold content and high porosity that contribute to further increase in the surface area of the fibers and consequent increase in the amount of DNA immobilized on the fibers. Fig. 5 also shows the result of sensing FPG with these fiber mats. Damage-specific detection of FPG is again observed, with detection at a similar threshold (~5 units/mL, 10 nM) and sensitivity over three orders of magnitude of glycosylase concentration. The extended dynamic range for the fibers probably arises because the surface access of DNA to the enzyme is likely much higher on the fibers (de Ávila et al., 2013). Thus, nanofibers also serve as suitable platforms for electrochemical monitoring of glycosylase activity.

4. Conclusion

The demonstration of an electrochemical measure of DNA repair at the level of the DNA is very beneficial for biological assays. As noted,

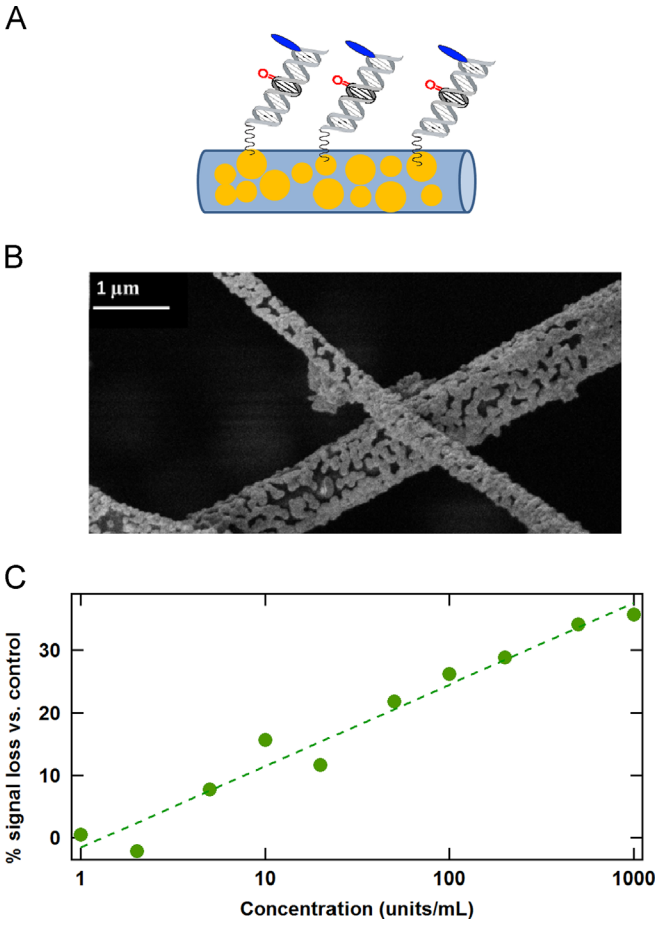

Fig. 5. (A) Illustration of the setup for detection of glycosylase activity with an electrospun nanofiber (not to scale). (B) SEM image of gold-bearing polyacrylonitrile nanofibers. (C) SW peak current signal loss of nanofiber-bound DNA monolayers containing 8-oxoguanine relative to an undamaged control versus concentration of FPG.

repair proteins often possess overlapping functionalities – in humans, multiple repair proteins recognize 8-oxoguanine. Our assay follows repair at the level of the damaged DNA and returns if repair occurs at all – by any protein. Device sensitivity on the order of femtomoles per electrode entails that sensing can be accomplished with even ~1 ng of enzyme. This sensitivity may be further improved with optimization of nanoscale devices, such as low cost nanofibers. Detection times are rapid, on the order of seconds, and in real time with the biological event. Damage-specific detection in a mixture of enzymes and in response to environmental oxidative damage was also demonstrated. Thus, this device approach achieves sensitive, selective, and rapid assay of repair protein activity, enabling a biological interrogation of DNA damage repair.

Acknowledgments

The authors would like to thank Chris Wohlgamuth, Kuo-Yao Lin and Kelly Jackson for their assistance. This work was performed in part at the UT Dallas Cleanroom Research Laboratory.

Appendix A. Supplementary material

Supplementary data associated with this article can be found in the online version at http://dx.doi.org/10.1016/j.bios.2013.11.034.

References

Abalea, V., Cillard, J., Dubos, M.-P., Sergent, O., Cillard, P., Morel, I., 1999. Free Radic. Bio. Med. 26 (11–12), 1457–1466.
Anka, F., Perera, S.D., Ratanatawanate, C., Balkus Jr., K.J., 2012. Mater. Lett. 75, 12–15.
Bellan, L.M., Craighead, H.G., 2011. Polym. Adv. Technol. 22 (3), 304–309.
Boal, A.K., Yavin, E., Lukianova, O.A., O'Shea, V.L., David, S.S., Barton, J.K., 2005. Biochemistry 44 (23), 8397–8407.
Boal, A.K., Barton, J.K., 2005. Bioconj. Chem. 16 (2), 312–32192.
Boon, E.M., Ceres, D.M., Drummond, T.G., Hill, M.G., Barton, J.K., 2000. Nat. Biotechnol. 18 (10), 1096–1100.
Boon, E.M., Salas, J.E., Barton, J.K., 2002a. Nat. Biotechnol. 20 (3), 282–286.
Boon, E.M., Pope, M.A., Williams, S.D., David, S.S., Barton, J.K., 2002b. Biochemistry 41 (26), 8464–8470.
Cahová-Kuchaříková, K., Fojta, M., Mozga, T., Paleček, E., 2005. Anal. Chem. 77 (9), 2920–2927.
Cash, K.J., Ricci, F., Plaxco, K.W., 2009. J. Am. Chem. Soc. 131 (20), 6955–6957.
David, S.S., O'Shea, V.L., Kundu, S., 2007. Nature 447 (7147), 941–950.
de Ávila, B.E.F., Watkins, H.M., Pingarron, J.M., Plaxco, K.W., Palleschi, G., Ricci, F., 2013. Anal. Chem. 85 (14), 6593–6597.
Dennany, L., Forster, R.J., White, B., Smyth, M., Rusling, J.F., 2004. J. Am. Chem. Soc. 126 (28), 8835–8841.
Gorodetsky, A.A., Boal, A.K., Barton, J.K., 2006. J. Am. Chem. Soc. 128 (37), 12082–12083.
Gorodetsky, A.A., Ebrahim, A., Barton, J.K., 2008. J. Am. Chem. Soc. 130 (10), 2924–2925.
Han, G., Guo, B., Zhang, L., Yang, B., 2006. Adv. Mater. 18 (13), 1709–1712.
Harfield, J.C., Toghill, K.E., Batchelor-McAuley, C., Downing, C., Compton, R.G., 2011. Electroanal 23 (4), 931–938.
Havran, L., Vacek, J., Cahová, K., Fojta, M., 2008. Anal. Bioanal. Chem. 391 (5), 1751–1758.
Ivandini, T.A., Honda, K., Rao, T.N., Fujishima, A., Einaga, Y., 2007. Talanta 71 (2), 648–655.
Kunkel, T.A., Erie, D.A., 2005. Annu. Rev. Biochem. 74, 681–710.
Kunduru, V., Bothara, M., Grosch, J., Sengupta, S., Patra, P.K., Prasad, S., 2010. Nanomed. Nanotech. Bio. Med. 6 (5), 642–650.
Liu, Z., Zhou, C., Zheng, B., Qian, L., Mo, Y., Luo, F., Shi, Y., Choi, M.M.F., Xiao, D., 2011. Analyst 136 (21), 4545–4551.
Luo, Y., Nartker, S., Miller, H., Hochhalter, D., Wiederoder, M., Wiederoder, S., Setterington, E., Drzal, L.T., Alocilja, E.C., 2010. Biosens. Bioelectron. 26 (4), 1612–1617.
Maehara, Y., Egashira, A., Oki, E., Kakeji, Y., Tsuzuki, T., 2008. Cancer Sci. 99 (3), 451–458.
Manesh, K.M., Kimb, H.T., Santhosh, P., Gopalan, A.I., Lee, K.-P., 2008. Biosens. Bioelectron. 23 (6), 771–779.
Marx, S., Jose, M.V., Andersen, J.D., Russell, A.J., 2011. Biosens. Bioelectron. 26 (6), 2981–2986.
Mugweru, A., Wang, B., Rusling, J., 2004. Anal. Chem. 76 (18), 5557–5563.
Mui, T.P., Fuss, J.O., Ishida, J.P., Tainer, J.A., Barton, J.K., 2011. J. Am. Chem. Soc. 133 (41), 16378–16381.
Obtułowicz, T., Sawoboda, M., Speina, E., Gackowski, D., Rozalski, R., Siomek, A., Janik, J., Janowska, B., Ciesla, M.J., Jawien, A., Banaszkiewicz, Z., Guz, J., Dziaman, T., Szpila, A., Olinski, R., Tudek, B., 2010. Mutagenesis 25 (5), 463–471.
Paleček, E., Bartošík, M., 2012. Chem. Rev. 112 (6), 3427–3481.
Paz-Elizur, T., Sevilya, Z., Leitner-Dagan, Y., Elinger, D., Roisman, L.C., Livneh, Z., 2008. Cancer Lett. 266 (1), 60–72.
Ravanat, J., Gremaud, E., Markovic, J., Turesky, R.J., 1998. Anal. Biochem. 260 (1), 30–37.
Rebelo, I.A., Piedade, J.A.P., Oliveira-Brett, A.M., 2004. Talanta 63 (2), 323–331.
Ren, G., Xu, X., Liu, Q., Cheng, J., Yuan, X., Wu, L., Wan, Y., 2006. React. Funct. Polym. 66 (12), 1559–1564.
Ricci, F., Bonham, A.J., Mason, A.C., Reich, N.O., Plaxco, K.W., 2009. Anal. Chem. 81 (4), 1608–1614.
Sancar, A., Lindsey-Boltz, L.A., Ünsal-Kaçmaz, K., Linn, S., 2004. Annu. Rev. Biochem. 73, 39–85.
Schibel, A.E.P., An, N., Jin, Q., Fleming, A.M., Burrows, C.J., White, H.S., 2010. J. Am. Chem. Soc. 132 (51), 17992–17995.
Shin, Y.J., Kameoka, J., 2012. J. Ind. Eng. Chem. 18 (1), 193–197.
Slinker, J.D., Muren, N.B., Gorodetsky, A.A., Barton, J.K., 2010. J. Am. Chem. Soc. 132 (8), 2769–2774.
Slinker, J.D., Muren, N.B., Renfrew, S.E., Barton, J.K., 2011. Nat. Chem. 3 (3), 228–233.
Wang, H., Peng, Z., Long, Y., Chen, H., Yang, Y., Li, N., Liu, F., 2012. Talanta 94, 216–222.
Wang, J., Rivas, G., Ozsoz, M., Grant, D.H., Cai, X., Parrado, C., 1997. Anal. Chem. 69 (7), 1457–1460.
White, R.J., Plaxco, K.W., 2010. Anal. Chem. 82 (1), 73–76.
Wohlgamuth, C.H., McWilliams, M.A., Slinker, J.D., 2013. Anal. Chem. 85 (3), 1462–1467.
Zhang, B., Guo, L.-H., Greenberg, M.M., 2012. Anal. Chem. 84 (14), 6048–6053.
Zhao, S., Guo, B., Han, G., Tian, Y., 2008. Mater. Lett. 62 (21–22), 3751–3753.
Zuo, X., Xiao, Y., Plaxco, K.W., 2009. J. Am. Chem. Soc. 131, 6944–6945.